

## A NUMERICAL STUDY ON THE EFFECTS OF LEADING-EDGE MODIFICATIONS UPON PROPELLER FLOW CHARACTERISTICS

**I.H. Ibrahim**

School of Mechanical and Aerospace Engineering  
Nanyang Technological University, 50 Nanyang Avenue, Singapore  
[imran.i@ntu.edu.sg](mailto:imran.i@ntu.edu.sg)

**T.H. New**

School of Mechanical and Aerospace Engineering  
Nanyang Technological University, 50 Nanyang Avenue, Singapore  
[dthnew@ntu.edu.sg](mailto:dthnew@ntu.edu.sg)

### ABSTRACT

This paper reports upon a numerical investigation into the implementation of tubercles in marine propellers. Although they have been mooted as a possible flow control solution in propeller designs, their exact implementation and performances have so far been virtually non-existent. In this work, global performance of a tubercle-modified propeller in terms of thrust and torque are determined from numerical simulations. These quantities are taken across various advance ratio values as well. Results show that implementation of tubercles on the propeller is able to improve thrust by up to 1.5%, specifically at lower advance ratio values. However, decreases in propeller efficiency are also observed. In particular, propeller efficiency only shows improvements above the baseline values when the advance ratio is 0.85 and beyond. Lastly, wall streamlines and surface pressure results are presented to shed light upon the influences exerted by the tubercles upon the propeller blade flow fields.

### INTRODUCTION

#### Propeller simulation studies

Optimizing blade geometries remains a challenge in the area of propeller design. One of the crucial design dilemmas surrounds the desire to have the propeller blades producing high thrust levels whilst maintaining satisfactorily low torques within desired geometrical constraints. With the advent of high performance computing and more realistic numerical schemes, the design of modern propellers has gradually shifted from analytical methods based on lifting-line or lifting-surface theories, to numerical methods that are based from discretizing the flow domain. This approach had developed rapidly from the 1960s onwards and seen increasing popularity. In particular, RANS-based numerical simulations have seen elevated adoption levels in the prediction of propeller performance, due to their satisfactory comparisons with experimental data. Furthermore, the use of a hybrid-unstructured mesh strategy in marine propeller simulations is also advocated by various researchers. For

example, Watanabe et al. (2003) performed RANS simulations on two different conventional propellers, where a hybrid mesh strategy consisting of tetrahedral cells was employed for easier generation. For studies involving steady, non-cavitating operating conditions, good agreements were observed between simulation results and experimental data. Rhee and Joshi (2006) utilized unstructured meshing on a P5168 propeller, where hybrid meshes were generated with sufficiently high boundary layer resolution on the blade and hub surface. Mesh adaptation was also initiated in the propeller wake region. The results indicated that global quantities such as thrust and torque agreed well with the measured values. Finally, a comparative mesh study had also been conducted by Morgut and Nobile (2012) to compare the effects of utilizing structured and hybrid meshing strategies on a propeller. Structured meshing techniques are known to be difficult and time-consuming to reproduce. While the results indicate that hybrid-unstructured meshes are less suited for detailed investigations of the flow field, for numerical predictions of the propeller open water characteristics, both meshing strategies can guarantee comparable levels of accuracy.

#### Tubercle Technology

The implementation of tubercles in aerofoils was motivated by observations first made by Fish and Battle (1995) on the movements of humpback whales. Humpback whales (*Megaptera Novaeangliae*) can grow up to 36 tons, but have high manoeuvrability as seen in Figure 1. Tubercles are essentially similar to wavy sinusoidal protrusions or periodic variations implemented on an aerodynamic surface. These protrusions create significant change to the aerodynamics, more significantly so as the geometry is tilted at higher angles of attack (Johari et al. (2007)). The flow changes are akin to strakes on aircraft which generate large vortices that change the stall characteristics of wings (Fish and Battle, 1995). The improvements seen in utilizing tubercles is a 3-D phenomenon that is both a function of the plan form geometry shape, as well as the Reynolds number (Miklosovic et al., 2007). Earlier authors concluded that

aerofoils with tubercles may have potential applications in lifting surfaces that are required to operate past their stall point, such as wind turbine blades. This is observed by changes in flow separation patterns and surface pressure distributions by adding tubercles at the leading-edge. Separation was delayed downstream of the tubercle crest (Weber et al., 2011) and vortices were produced and re-energized the boundary layer by carrying high-momentum flow close to the flipper's surface.

Johari et al. (2007) conducted experimental research on the effects of tubercles on a NACA 634-021 aerofoil profile. Tubercle amplitudes and spanwise wavelengths are varied in the design of the tubercles. The results indicated that in the pre-stall regime, protuberances caused a reduction in the lift coefficient. However, drag penalties were also incurred. In the post-stall regime, protuberances on the leading-edge resulted in higher lift coefficients, by as much as 50%, with negligible drag penalties. The main finding of the research was that tubercles amplitude has a more significant effect on resulting forces and moments, as compared to the wavelength. The flow over the protuberances remained attached well past the stall angle of the baseline aerofoil. Also, flow separation at the leading-edge of modified foils occurred mainly only in the troughs between the adjacent protuberances.

The success of deploying tubercles as a flow control device can be seen by their implementation onto commercial industrial fans, or High-Volume Low-Speed (HVLS) fans. Envira-North Systems Ltd. produces the HVLS fans for large buildings (e.g., factories, warehouses, arenas, dairy barns, etc.) incorporated with leading-edge tubercles designed by Whalepower Corporation. In addition to being 25% more efficient, the HVLS fan is also 20% quieter as compared to conventional ceiling fans. Note that the suppression of tonal noise by the addition of tubercles to an aerofoil was observed in a low-speed wind tunnel before (Hansen et al., 2012), where tonal noise was found to be most effectively reduced by tubercles of large amplitude ( $\delta$ ) and smaller wavelength ( $l$ ).

Another interesting implementation of tubercles to a fan can be seen in the commercially available 'Bionic' CPU fan, designed to reduce the noise levels in a computer system (Evologics, 2014). The dimensions of the fans are in the scale of ~100mm, with protuberances incorporated along the leading-edges of the blades, similar to the fundamental designs employed in the current work.

However, in view of the lack of hard scientific data, it would appear that the primary motivation for this design was noise reduction, rather than flow optimisations. It is from these observations that the basis of the present bio-inspired propeller study is derived: to explore tubercles as a potential passive flow control/enhancement device so as to prevent flow separations at higher angles of attack, thereby increasing the stall angle, creating larger advance ratios ( $J$ ) and eventually, better propeller performance. The applications thus far highlight the use of tubercles only in a single-axis curvature form. As the marine propeller blade

consists of sections with varying pitch angles, the effectiveness of implementing the tubercles will no doubt be tested. The methodology of designing the modified blades will be described next.



Figure 1. Left: The Humpback Whale (*Megaptera Novaeangliae*). Right – Close-up of the pectoral fin with tubercles. Picture adapted from (Fish et al., 2011).

## METHODOLOGY

### Blade design

The baseline and modified propellers are 375mm in diameter and are shown in Figure 2. The propeller consists of three blades and a circular hub which tapers at the pressure side of the blades. The modified blades are designed with two important design constraints: maintenance of the downstream aerofoil profile, as well as conservation in blade area with respect to the baseline model. As a preliminary design for the present study, the tubercle wavelength and amplitude are kept at 25% and 2.5% of the mean blade chord length respectively. The mean chord length is defined as the averaged chord lengths of the aerofoil sections along the blade and estimated to be 80mm. Figure 2 shows that the selected modifications result in blades consisting of six pairs of crests and troughs each.

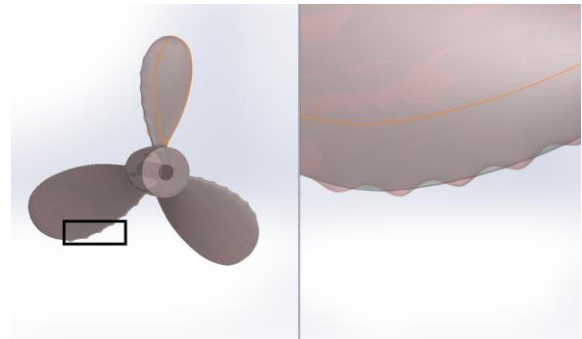


Figure 2. The baseline (grey) and modified (light brown) propellers superimposed and shown at the propeller suction side (left) and zoomed (right). The crests of the tubercles protrude above the baseline propeller leading edge indicating conservation in planform areas.

### Numerical technique

The specifications of the simulation domain size are shown in Figure 3. The size of the simulation domain were

deemed large enough to result in negligible change in the open water characteristics results based on investigations previously conducted. A periodic simulation was also not utilized as a full propeller simulation did not incur significant computational costs.

The numerical predictions presented in this work were performed by Fluent 15 (ANSYS®-Academic-Research, 2013). The Multiple Reference Frame (MRF) approach was applied in the simulation of the marine propeller. The propeller is placed within a subdomain called the *Rotating* domain, while the remaining portions were stationary or *Fixed*. Due to the large difference in impeller size relative to the simulation domain, the absolute velocity formulation was selected. The governing equations for fluid flow for a steadily moving frame can be written as follows:

Mass conservation:

$$\nabla \cdot \rho \vec{v}_r = 0 \quad (1)$$

Momentum conservation:

$$\nabla \cdot (\rho \vec{v}_r \vec{v}) + \rho [\vec{\omega} \times \vec{v}] = -\nabla p + \nabla \cdot \vec{\tau} + \vec{F} \quad (2)$$

where

$\rho$  = Density (kg/m<sup>3</sup>) = 998.2 kg/ m<sup>3</sup>

$\vec{v}$  = Absolute velocity (m/s)

$\vec{v}_r$  = Relative velocity (m/s)

$\vec{\omega}$  = Angular velocity (rad/s)

$\vec{\tau}$  = Viscous stress

$\vec{F}$  = Body force

The inlet, outlet and outer boundaries of the *Fixed* part were located at a distance which were large enough that would dispel any changes to the solution. The inlet boundary condition having a turbulence intensity of 5% and a normal free stream velocity component of 2 m/s. A zero Pascal static pressure was imposed at the outlet boundary. A no-slip boundary condition was applied to the propeller wall.

The realizable k-ε model with Enhanced Wall Treatment (EWT) was utilized as a turbulence model in this work. The key reasons in using the k-ε model are robustness, economy and reasonable accuracy for a wide range of turbulent flows. The realizable model is recommended relative to other variants of the k-ε family because of the improvements shown where the flow features include strong streamline curvature, vortices, and rotation. The EWT specification is also utilized in conjunction with the k-ε model. The EWT is a near-wall modelling method that combines a two-layer model with enhanced wall functions. This method is effective in combining the accuracy of a standard two-layer approach for fine near-wall meshes as well as conservative analysis for wall-function meshes.

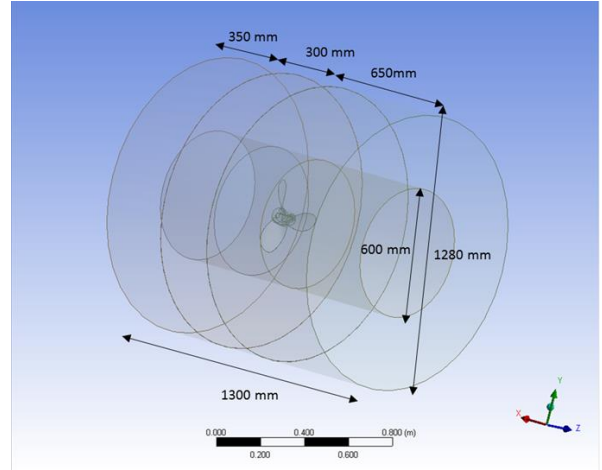


Figure 3. Simulation domain size used in the analysis.

## Mesh analysis

A mesh convergence study was conducted on the baseline propeller to ensure the use of appropriately-sized mesh size. Three different mesh settings were utilized and henceforth named 'Coarse', 'Medium' and 'Fine'. The average  $y^+$  value calculated for the baseline propeller blade and hub is 37, while the average  $y^+$  values for the modified propellers lie in the range of 20~30. The thrust and torque characteristics were relatively similar for the three grid settings with minor differences. To better highlight their differences, the results are presented in percentages relative to the baseline propeller curves in Figure 4.

The results indicate that in terms of thrust, the trends obtained for the 'Medium' and 'Fine' cases are almost identical, with predicted thrust levels of between 3.5% and 11% lower than towing tank results for  $J=0.4$  to  $0.9$ . As for the torque results, the 'Medium' grid setting recorded a moderate difference of between -3% and 2% for the same advance ratio range. Based from the results, the 'Medium' grid setting was deemed to be most appropriate for the present simulations. Furthermore, simulation and towing tank results for thrust and torque coefficients are shown in Figure 5 and good agreements can be inferred from the comparison. Lastly, a close-up grid view of the propeller blade for the 'Medium' setting is shown in Figure 6. The 'wall' boundary condition employed to the propeller has been inflated with regular prismatic meshes to adequately resolve boundary layer growth. The hybrid meshing approach have been defined by the following: the *Rotating* domain has been resolved with unstructured tetrahedral and prismatic mesh, while the remaining *Fixed* domains are swept with regular hexahedral meshes.

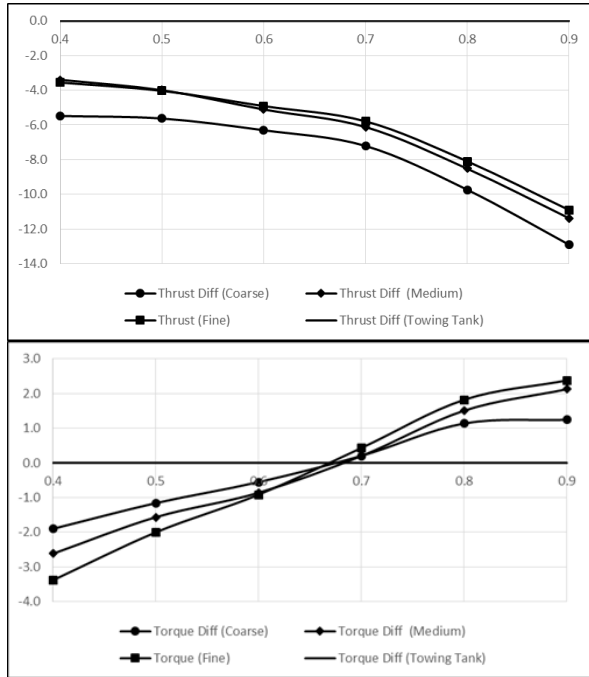


Figure 4. Differences in thrust (top) and torque (bottom) as a percentage to the baseline propeller curves.

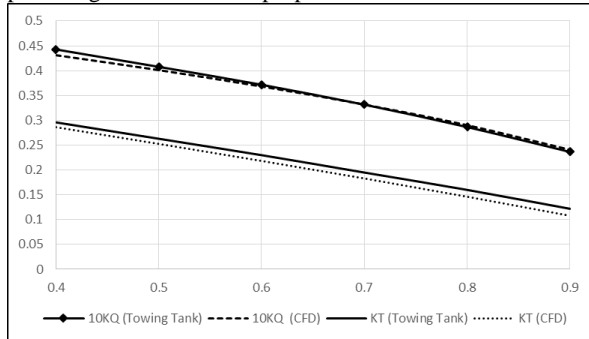


Figure 5. Thrust and torque coefficients for the simulation and towing tank experiment.

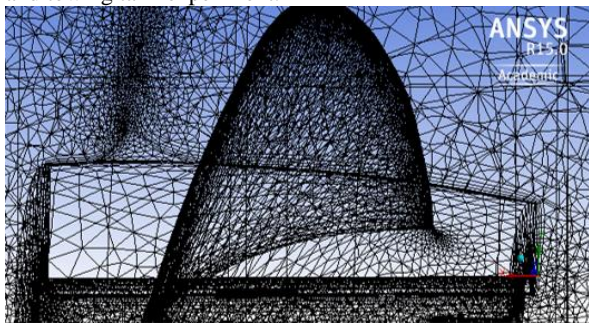


Figure 6. Mesh view near of the propeller showing the hub and blade.

## RESULTS

For the flow simulations conducted, metrics typically determined to assess the performance of the marine

propellers will include thrust, torque, advance ratio and propeller efficiency. The forces and moments produced by the marine propeller are expressed in their most fundamental forms as non-dimensional coefficients, defined here as:

$$\text{Thrust Coefficient: } K_T = \frac{T}{\rho n^2 D^4} \quad (3)$$

$$\text{Torque Coefficient: } K_Q = \frac{Q}{\rho n^2 D^5} \quad (4)$$

$$\text{Advance Ratio: } J = \frac{V_a}{nD} \quad (5)$$

$$\text{Efficiency: } \eta = \frac{K_T J}{K_Q 2\Pi} \quad (6)$$

where

$T$  = Thrust (N)

$n$  = Rotational speed (rps)

$D$  = Propeller diameter (m) = 0.375 m

$V$  = Characteristic velocity of flow (m/s) = 2 m/s

## Thrust, Torque and Efficiency

Simulation results for the modified and baseline propellers are plotted in Figure 7. The results show that implementing the tubercles to the propeller improves thrust coefficient to about 1.5%, specifically at lower advance ratio values. However, this results in an increase in torque of about 6% and therefore a decrease in propeller efficiency. The results also suggest that the propeller efficiency increases with higher advance ratios and that the efficiency of the modified propeller exceeds that of the baseline propeller at  $J=0.85$ . To fully understand the results of the open-water propeller characteristics, examination of the near-wall flows, for instance, the nature of the flow close to the blade surface, boundary layer separation and corresponding flow structures will be shown in the next subsection.

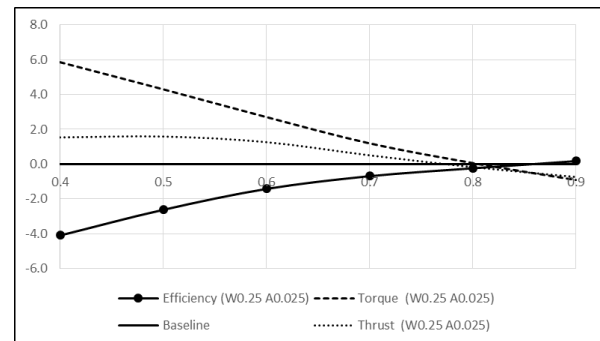


Figure 7. Percentage differences in performance metrics of the modified propeller compared to the CFD baseline design results as denoted as the x-axis.

## Wall shear streamlines

Wall shear streamlines provide indications of particle flow direction along the blade surface, where longer

streamlines indicate attached flows along the vicinity of the propeller blade. With that in mind, the wall shear streamlines for the baseline and modified propellers at  $J=0.9$  and  $J=0.4$  are shown in Figure 8 and Figure 9 respectively. As an indication of the fluid flow direction, note that the bottom edge of the propeller is the leading-edge.

The results show that the streamlines along the baseline propeller blade are virtually parallel to one another, except at the blade root and tip regions. At the blade tip vicinity, the streamlines meander in the radial direction towards blade tip. The meandering becomes more discernible for the modified propeller at  $J=0.4$ , particularly at the central trough and the trough closest to the blade tip. For the modified blades, the streamlines appear to consolidate more closely at the peaks than the troughs, suggesting enhanced flow separation behaviour at the troughs of the tubercles

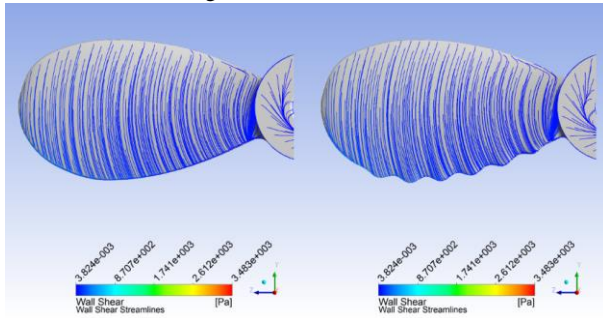


Figure 8. Wall shear streamlines for a baseline (left) and modified (right) propeller blade at  $J=0.9$ .

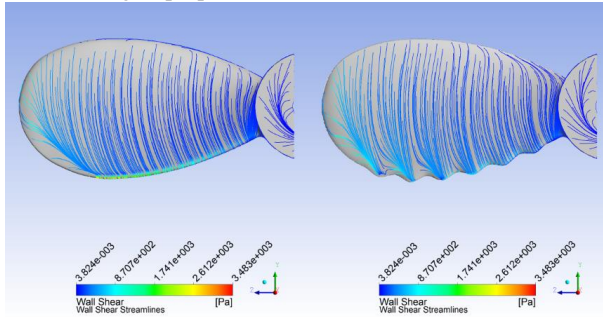


Figure 9. Wall shear streamlines for a baseline (left) and modified (right) propeller blade at  $J=0.4$ .

### Blade surface pressure

The surface pressure contours at the suction side of the baseline and modified propellers at  $J=0.9$  and  $0.4$  are now shown in Figure 10 and Figure 11 respectively. The surface pressure distributions of the blades provide some correlation with the forces acting on the blade, which is in turn associated with the resulting thrust. The contours are generally similar for both baseline and modified propellers at a high advance ratio of  $J=0.9$ , but higher pressure regions seem to exist at the peaks of the tubercles. At  $J=0.4$  however, the tubercles closer to the blade root disrupts the low pressure uniformity that had been present in the baseline propeller. This results in comparatively larger low pressure

regions to exist at the trough accompanying the last tubercle. The resulting increased non-uniformity in the surface pressure distribution along the leading-edge is now significantly more apparent.

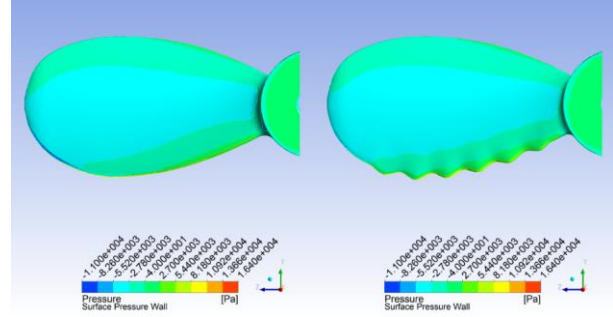


Figure 10. Surface pressure for a baseline (left) and modified (right) propeller blade at  $J=0.9$ .

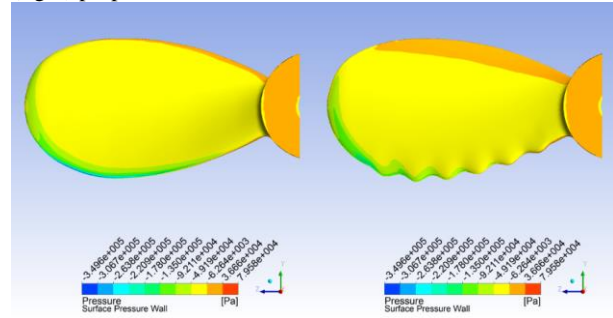


Figure 11. Surface pressure for a baseline (left) and modified (right) propeller blade at  $J=0.4$ .

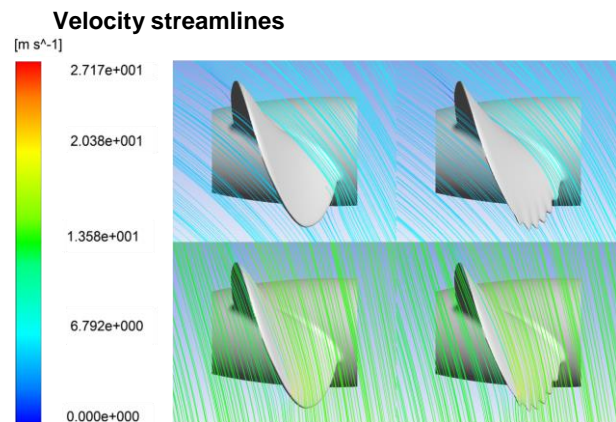


Figure 12. Surface velocity streamlines for the baseline and modified propellers at  $J=0.4$  positioned near root (top) and tip (bottom) of the blades.

The velocity streamlines for both baseline and modified tubercles running at  $J=0.4$  in Figure 12. They are surface streamlines positioned near the root and tip of the blades. The lack of recirculating streamlines indicates the absence of significant flow separations near the propeller blades. This suggests that, at the range of advance ratios tested, the

aerofoil profiles along the blade section are effectively inclined at low angles-of-attack relative to the incoming flow at these advance ratios. This also implies that the combinations of Reynolds numbers and the effective (Angle of Attack) AOA apparent to the blade leading-edges are too low to induce flow separation.

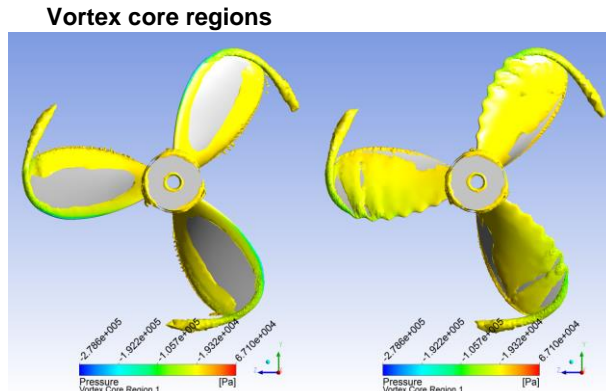


Figure 13. Vortex core regions for the baseline (left) and modified (right) propellers at  $J=0.4$ .

The vortex core implementation is a special type of isosurface that displays a vortex. It is based from the Q-criterion as described by Q-criterion index introduced by Hunt, Wray and Moin (Hunt et al., 1988). The formulation is as follows:

$$Q = \frac{1}{2} [\Omega^2 - S^2] \quad (7)$$

where  $\Omega$  and  $S$  is the vorticity and strain rate tensors respectively.

The vortical wake structures for both the baseline and modified propellers in Figure 13 can be divided into two main parts; the vortex core generated at both the leading edge of the blade, as well as the blade tip vortices. The vortex sheet remains attached for the modified blade but separates at midstream for the baseline blade. A vortex sheet also appears to form at the final trough of the modified blade.

## CONCLUSION

Implementation of tubercles upon a marine propeller shows improvements to thrust of up to 1.5% at lower advance ratio values. However, propeller efficiency also decreases at low advance ratios. Results suggest that the propeller efficiency only increases with increasing advance ratios and that the efficiency of the modified propeller exceeds that of the baseline propeller at  $J=0.85$ . The differences in the performance metrics for the baseline and modified propeller are found to be relatively small. One likely reason is that the combinations of Reynolds numbers and the effective AOA's apparent to the blade leading-edges are too low to induce flow separation.

As a future study, It may be possible to use the isosurface plots to predict the extent of the cavitation regions. However, this would require careful calibration of the Q value for accurate and optimal predictions. Although no cavitation is observed for the baseline propeller in open water tests (and modelled as such in the present study), it remains to be seen whether the tubercles would induce this phenomena at higher operating speeds, particularly at the sharp edges of the crests.

## ACKNOWLEDGEMENT

The authors gratefully acknowledge the support of the present study by DSO National Laboratories (Singapore).

## REFERENCES

- ANSYS®-Academic-Research (2013). ANSYS Fluent User's Guide Release 15.0.
- Evologics. (2014). "Evologics." from <http://www.evologics.de/en/products/propeller/index.html>.
- Fish, F. E. and J. M. Battle (1995). "Hydrodynamic design of the humpback whale flipper." *Journal of Morphology* **225**(1): 51-60.
- Fish, F. E., P. W. Weber, M. M. Murray and L. E. Howle (2011). "The tubercles on humpback whales' flippers: Application of bio-inspired technology." *Integrative and Comparative Biology* **51**(1): 203-213.
- Hansen, K., R. Kelso and C. Doolan (2012). "Reduction of flow induced airfoil tonal noise using leading edge sinusoidal modifications." *Acoustics Australia* **40**(3): 172-177.
- Hunt, J. C., A. Wray and P. Moin (1988). *Eddies, streams, and convergence zones in turbulent flows*. Studying Turbulence Using Numerical Simulation Databases, 2.
- Johari, H., C. Henoeh, D. Custodio and A. Levshin (2007). "Effects of leading-edge protuberances on airfoil performance." *AIAA Journal* **45**(11): 2634-2642.
- Miklosovic, D. S., M. M. Murray and L. E. Howle (2007). "Experimental evaluation of sinusoidal leading edges." *Journal of Aircraft* **44**(4): 1404-1408.
- Morgut, M. and E. Nobile (2012). "Influence of grid type and turbulence model on the numerical prediction of the flow around marine propellers working in uniform inflow." *Ocean Engineering* **42**: 26-34.
- Rhee, S. H. and S. Joshi (2006). "Computational validation for flow around a marine propeller using unstructured mesh based Navier-Stokes solver." *JSME International Journal, Series B: Fluids and Thermal Engineering* **48**(3): 562-570.
- Watanabe, T., T. Kawamura, Y. Takekoshi, M. Maeda and S. H. Rhee (2003). *Simulation of steady and unsteady cavitation on a marine propeller using a RANS CFD code*. Fifth International Symposium on Cavitation, Osaka, Japan.
- Weber, P. W., L. E. Howle, M. M. Murray and D. S. Miklosovic (2011). "Computational evaluation of the performance of lifting surfaces with leading-edge protuberances." *Journal of Aircraft* **48**(2): 591-600.